

²Yu. M. Aliev *et al.*, Phys. Rev. A **15**, 2120 (1977).
³H. Hora, Phys. Fluids **12**, 182 (1969); J. Dawson *et al.*, Phys. Fluids **12**, 875 (1969). R. E. Kidder, in *Proceedings of the Japan-U. S. Seminar on Laser Interaction with Matter, Kyoto, Japan, 1972*, edited by K. Yamana (Japan Society for the Promotion of Science, Tokyo, 1973).
⁴N. G. Denisov, Zh. Eksp. Teor. Fiz. **31**, 609 (1956) [Sov. Phys. JETP **4**, 544 (1971)]; V. L. Ginsberg, *The Propagation of Electromagnetic Waves in Plasmas*, (Addison-Wesley, Reading, Mass., 1969), pp. 193-228;

J. D. Lindl and P. K. Kaw, Phys. Fluids **14**, 371 (1971); R. K. Osborn, IEEE Trans. Plasma Sci. **3**, 116 (1975); White and Chen, Ref. 1.
⁵P. Mulser and C. van Kessel, Phys. Rev. Lett. **38**, 902 (1977).
⁶K. A. Brueckner, and R. J. Janda, Nucl. Fusion **17**, 451 (1977); J. Virmont *et al.*, to be published.
⁷K. Lee *et al.*, Phys. Fluids **20**, 51 (1977).
⁸L. M. Brekhovskikh, *Waves in Layered Media* (Academic, New York, 1960).
⁹I. P. French *et al.*, Can. J. Phys. **39**, 1273 (1961).

High-Energy Ion Expansion in Laser-Plasma Interactions

R. Decoste

University of Maryland, College Park, Maryland 20742

and

B. H. Ripin

Naval Research Laboratory, Washington, D. C. 20375

(Received 18 July 1977)

Measurements of energetic-ion energy distributions produced from CD₂ and CH₂ targets are compared with a numerical model. The model describes the ambipolar expansion of hot electrons and two relatively cold ion species from an electron pressure gradient. For CD₂ the plasma expansion is adequately represented by a single ion species, whereas for CH₂ two-ion fluids are required to account for the energy and the relative behavior of the high-energy ion species.

Historically, the high-energy ions in a laser-produced plasma are defined as a small group of ions transporting a significant fraction of the absorbed laser energy. Most expansion models^{1,2} indicate that the energetic ions are the direct consequence of the presence of high-energy electrons. Most plasma simulations^{1,3} use a single ion species to model the ion expansion. Here we show that, although the hot-electron expansion can account for the energy content of the fast ions, a multi-ion-species description is usually required to reproduce the measured high-energy ion distributions. Ion energy distributions measured from CD₂ targets, where both predominant species, C⁶⁺ and D⁺, have the same charge-to-mass ratio, are adequately represented by a single-ion-species expansion. For CH₂ targets, however, a two-ion fluid description is required to reproduce the qualitative features of the ion expansion.

Typical single-shot energy distributions of high-energy ions from Nd-laser irradiation (75 psec, ~10¹⁶ W/cm² with an *f*/2 lens) of CD₂ and CH₂ thick-slab targets are shown in Figs. 1 and 2, respectively. The gross variations between the

charge-collector oscilloscope traces such as shown in Figs. 1(b) and 2(b) are mainly due to the different viewing angle between the target normal and the analyzer axis. For both cases the analyzer axis was at 35° with respect to the laser axis but the target normals in Figs. 1 and 2 were 35° and 22°, respectively, from the laser axis toward the analyzer. The high-energy-ion electrostatic analyzer⁴ used has twelve channels with 10% species and energy resolution. Since this analyzer cannot resolve C⁶⁺ from D⁺ ions, the C⁶⁺ were removed by allowing them to charge exchange with a nitrogen background gas (1.5 × 10⁻⁴ Torr) in the target chamber before entering the ion analyzer. The lowered ionization stages, originally C⁶⁺, can then be differentiated from D⁺ ions. The ion energy distribution is finally reconstructed from the summation of the recombination products. For either CH₂ or CD₂ targets no ionization stages lower than C⁵⁺ and only a small fraction of C⁵⁺ appeared under good vacuum conditions (8 × 10⁻⁷ Torr).

The multipeak structures on the H⁺ and D⁺ energy distributions were always observed but were nonreproducible in detail.^{4,5} The main difference

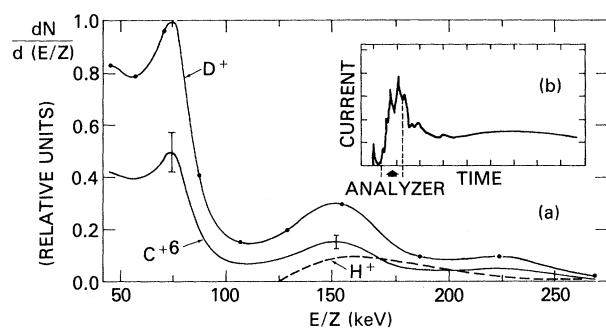


FIG. 1. (a) High-energy-ion distributions from CD_2 planar target. The number of H^+ is consistent with a 3% hydrogen concentration measured in the CD_2 material. (b) Oscilloscope trace from a biased charge collector showing the portion of the trace sampled by the ion analyzer.

between the two targets is in the relative behavior of the C^{6+} energy distribution with respect to the H^+ or D^+ distribution. For the CD_2 target, the ratio of the number of D^+ to C^{6+} remains approximately constant with increasing E/Z (energy divided by the charge). For the CH_2 target, however, little correlation was found between the C^{6+} and H^+ peaks but the average ratio of H^+ to C^{6+} was increasing with E/Z . In fact, above 50 keV/Z, more than half the fast-ion energy was transported by H^+ .

Figure 1 suggests that the plasma expansion from the CD_2 target behaves like a single ion species during the acceleration phase of the expansion. The relative behavior of D^+ and C^{6+} should therefore be predictable from a single-particle model. From the equation of motion of an ion accelerated in an electric field \mathcal{E} the rate of change of ion kinetic energy ($E_i = \frac{1}{2}m_i v_i^2$) is given by

$$\frac{d E_i}{dt} = \frac{Z_i e^2}{A_i m_p} \mathcal{E}^2 t, \quad (1)$$

where A_i and Z_i are, respectively, the atomic number and charge state of the ion. From Eq. (1), only the ion species with the same A/Z acquire the same E/Z regardless of the spatial or temporal dependence of the electric field. Both C^{6+} and D^+ have an A/Z of 2. Figure 1 also shows that CD_2 targets yield C^{6+} and D^+ with the same E/Z behavior. This leads to the conclusion that most of the carbon ions were already fully ionized before the acceleration phase. A mixture of ionization stages lower than C^{6+} could not give the same E/Z for C^{6+} and D^+ if the carbon ions were stripped during or after acceleration. A

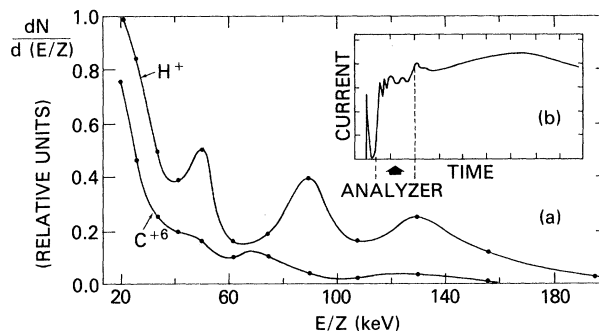


FIG. 2. (a) High-energy-ion distributions for a CH_2 target. (b) Oscilloscope trace from a biased charge collector showing the portion of the trace sampled by the ion analyzer.

CD_2 target can therefore be adequately represented by a single ion species.

For a CH_2 target, Eq. (1) can be used for the case of different ion species accelerated through a static potential sheet for *different* acceleration times,⁶ i.e., $t \propto (A_i/Z_i)^{1/2}$. Under this assumption, C^{6+} and H^+ should still have the same E/Z behavior. Figure 2, however, contradicts the static-potential assumption since an important fraction of the H^+ are accelerated to an E/Z larger than the C^{6+} . A second approach is to assume that the expansion of the faster H^+ ions decreases the electric field strength such that the acceleration time and the electric field are essentially the *same* for both C^{6+} and H^+ . The final energy relationship between C^{6+} and H^+ is then ideally given by

$$(E_i/Z_i)(A_i/Z_i) = \text{const.} \quad (2)$$

Equation (2) basically says that H^+ are expected at a higher E/Z than the C^{6+} , in qualitative agreement with the experimental results (Fig. 2).

For a CH_2 target a multifluid description of the plasma expansion is more appropriate than the single-particle model discussed earlier. Therefore, we model a one-dimensional ambipolar plasma expansion with a hot-electron background and two relatively cold ion fluids. The ion density profiles for our initial-value problem are shown in Fig. 3(a) (dashed lines). Both C^{6+} and H^+ density profiles have initially the same exponential scale length and a velocity negligible with respect to the final velocities. The three species, one electron and two ions, are described by the standard set of fluid equations.² Each ion fluid satisfies a continuity equation. The momentum equation for the hot electrons is a stress balance between the electron pressure

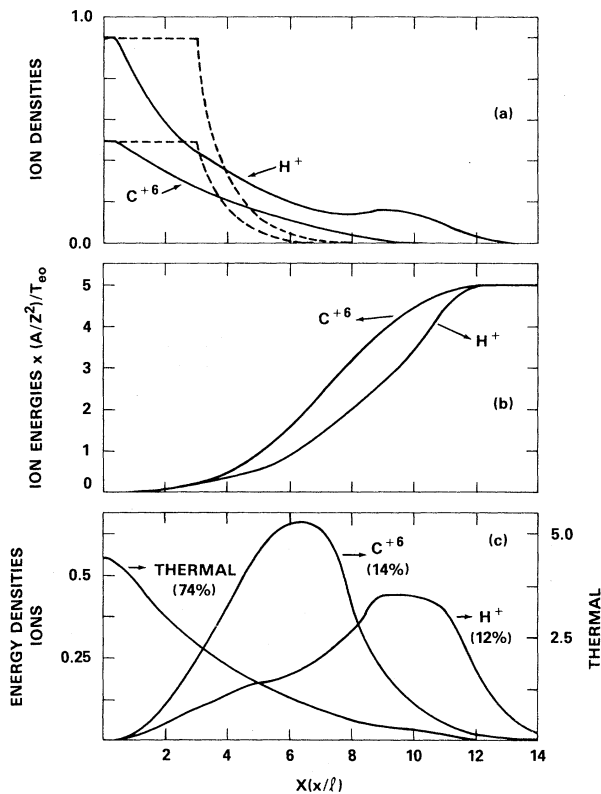


FIG. 3. Ion densities, ion energies, and energy densities vs distance at $t = 3.6\tau$. The dashed lines represent the initial density profiles. The ion densities are normalized to the initial H^+ plateau density. The non-dimensional units are $\tau = l/c_s$, $c_s = (kT_{e0}/m_p)^{1/2}$, where T_{e0} is the initial electron temperature and l the initial density-gradient scale length. The percentage in parentheses gives the energy partition.

gradient and the ambipolar electric field. We also assume that the density-gradient scale length is much greater than the electron Debye length and therefore replace the Poisson equation for the ambipolar potential by a quasineutrality condition $n_e = Z_1 n_1 + Z_2 n_2$.

The only interaction between the two ion species is through the self-consistent electric field in the momentum equations for the ions. No collisional effects have been included in this model. Electron-ion collisions can be neglected because of the high electron temperature. An initial ion temperature⁷ of a few hundred eV also makes the viscosity term ($\propto T_i^{-3/2}$) negligible with respect to the ambipolar electric field.^{8,9} The ion temperature, although high enough to neglect viscosity, remains relatively small compared to the electron temperature, so that the ion pressure can also be neglected.

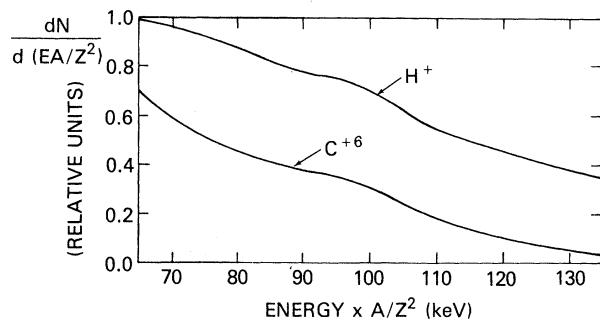


FIG. 4. Asymptotic high-energy-ion distributions calculated from Fig. 3 using a 30-keV initial electron temperature.

An assumption about the electron temperature and the heat flow is required to close the momentum equations. For the case presented in Fig. 3, a uniform electron temperature throughout the expansion region was assumed, i.e., the heat is allowed to flow without inhibition. The left boundary in Fig. 3(a) is an impenetrable wall. The total energy is then conserved by reducing the electron temperature according to the rate of change of ion kinetic energy. Other heat-flow assumptions such as an adiabatic expansion² or a strongly inhibited heat transport (flux limiter)¹ have also been used, yielding no fundamental differences in the qualitative features that will be discussed below. Our two-fluid model is therefore not a strong test of the validity of the isothermal expansion assumption.^{3,10}

The set of fluid equations has been solved numerically using an FCT algorithm¹¹ on a sliding-zone grid. Figure 3(a) shows the evolution of the ion density profiles for a CH_2 plasma after 3.6τ (where τ is the density-gradient scale length divided by the hydrogen-ion sound speed). As can be seen from Figs. 3(b) and 3(c), most of the ion expansion energy is contained in a small fraction of the ions with energies higher than the initial electron temperature. About 75% [Fig. 3(c)] of the electron thermal energy remains after 3.6τ but, because of the much weaker density gradient, ion acceleration by the ambipolar electric field is greatly reduced. The ion acceleration time is therefore approximately the same for both C^{6+} and H^+ . The remaining thermal energy will be dissipated via channels other than fast-ion production.

The asymptotic energy distributions, calculated from Fig. 3, are shown in Fig. 4 assuming an initial electron temperature of 30 keV. The ratio of H^+ to C^{6+} is increasing with ion energy, in

qualitative agreement with the measured energy distributions. Other initial density profiles have also been tried in the model and these affected the detailed shape of the asymptotic ion energy distribution. However, in all cases, a significant fraction of the H^+ was always observed at higher E/Z than the C^{6+} . From Fig. 3, one can see that, although the ion acceleration time was about the same for both ion species, the electric field was not. The H^+ , being faster, can get to the stronger-electric-field region and take advantage of the pressure gradient set up by the slower-moving C^{6+} . Since the accelerating electric field is different for the two species Eq. (2) is not quite valid and more H^+ are found at higher EA/Z^2 than C^{6+} in Fig. 4.

The typical ion-acceleration time scale for an initial electron temperature of ~ 30 keV and scale length of a few microns is a few tens of picoseconds. This relatively high electron temperature has then to be maintained for only a short time and is therefore a peak temperature consistent with other simulations.^{1,7,12} The multipeak structure on the ion energy distributions is not reproduced by our model. However, temporal variations of the pressure gradient on the time scale mentioned above could give bursts of ions of decreasing energies.

In summary, the electron-pressure-gradient model can account for the energy and the relative behavior of high-energy ion species. Furthermore, it was also shown that for some plasmas (CD_2 , for example) a single-ion-species description is quite adequate to simulate the plasma expansion although, for others, a multispecies description is required. The determining criterion is whether all the ions have the same A/Z during the expansion. A CH_n target can never have the same A/Z . Caution should also be used with targets made from higher- Z material (glass, Al, etc.) of unknown degree of ionization during the expansion. The mixture of different ion species

results in a preferential acceleration of the lower- A/Z ions by the higher- A/Z ions.

The authors wish to thank S. E. Bodner, H. R. Griem, F. S. Felber, and I. B. Bernstein for their interesting comments on this work and D. G. Colombant for his valuable assistance in the numerical calculations. This research was performed at NRL under the auspices of the U. S. Energy Research and Development Administration. One of the authors (R.D.) acknowledges receipt of a Hydro-Quebec fellowship (Canada).

¹R. C. Malone, R. L. McCrory, and R. L. Morse, *Phys. Rev. Lett.* **34**, 721 (1975).

²E. J. Valeo and I. B. Bernstein, *Phys. Fluids* **19**, 1348 (1976).

³P. M. Campbell, R. R. Johnson, F. J. Mayer, L. V. Powers, and D. C. Slater, *Phys. Rev. Lett.* **39**, 274 (1977).

⁴R. Decoste and B. H. Ripin, *Rev. Sci. Instrum.* **48**, 232 (1977).

⁵R. Decoste and B. H. Ripin, *Appl. Phys. Lett.* **31**, 68 (1977). R. Perkins, in *Proceedings of the IEEE 1977 Conference on Plasma Science* (IEEE, New York, 1977).

⁶A. W. Ehler, *J. Appl. Phys.* **46**, 2464 (1975).

⁷B. H. Ripin *et al.*, *Phys. Rev. Lett.* **34**, 1313 (1975).

⁸A regime of target irradiances for which the viscosity was dominant has been considered a few years ago by P. Mulser, *Plasma Phys.* **13**, 1007 (1971).

⁹An effective cooling of the ions during expansion by a strong ambipolar electric field has been described by A. V. Gurevich, L. V. Partiskaya, and L. P. Pitaevskii, *Zh. Eksp. Teor. Fiz.* **49**, 647 (1965), and **63**, 516 (1973) [*Sov. Phys. JETP* **22**, 449 (1966), and **36**, 274 (1973)]. The resulting increase in viscosity is partly offset by a reduction of the ion density during the expansion.

¹⁰J. E. Crow, P. L. Auer, and J. E. Allen, *J. Plasma Phys.* **14**, 65 (1975).

¹¹For this FCT (flux-corrected transport) algorithm, see J. P. Boris and D. L. Book, *J. Comput. Phys.* **11**, 38 (1973).

¹²R. S. Craxton and M. C. Haines, *Phys. Rev. Lett.* **35**, 1336 (1975).